Spring 2015

Thermographic investigation of laser metal deposition

Sreekar Karnati

Department:

THERMOGRAPHIC INVESTIGATION OF LASER METAL DEPOSITION

by

SREEKAR KARNATI

A THESIS

Presented to the Faculty of the Graduate School of the

MISSOURI UNIVERSITY OF SCIENCE AND TECHNOLOGY

In Partial Fulfillment of the Requirements for the Degree

MASTER OF SCIENCE IN MECHANICAL ENGINEERING

2015

Approved by

Frank W Liou, Advisor
Joseph W Newkirk
Edward C Kinzel

ABSTRACT

Laser metal deposition as an additive manufacturing technique has been proven to possess the capability for fabricating complex, intricate geometries and excellent material properties through material deposition. Accurate manufacture of such geometric features would require precise control over the material deposition process. The need of the hour are process monitoring and analyses mechanisms that are crucial in ascertaining the occurrence of the intended actions during deposition while also serving as effective learning tools. The current work involved developing and incorporating an Infra-Red (IR) camera as a process monitoring tool for laser metal deposition. Using the IR camera the thermal dynamics of the deposition processes under the control of the feedback systems were captured and analyzed to realize the changes in the material close to solidus temperature. The analysis confirmed the logic behind the control system and was successful in helping identify the ideal process parameters which were quantified using a set of experiments. The sub-sequent effort was focused on further disseminating thermographic data to attain details about the material above the solidus temperature. Employing image processing techniques pertaining to edge detection, regions that encompass the material above the solidus temperature were successfully identified. IR camera data was also used to track the regions of interest through the deposition and make other characteristic observations pertaining to phase change. To further test the sensitivity of this technique a series of experiments with varying power, track length and substrate size were performed. The developed methodology proved successful in identifying the regions of interest with a high degree of sensitivity and repeatability. Comprehensive insights into the physics of the process were also successfully obtained.

ACKNOWLEDGMENTS

The current work is an outcome of support and encouragement from the following people. I am immensely grateful to Dr. Frank Liou for accepting me into LAMP lab and providing this opportunity. I am thankful for the guidance and exposure Dr. Liou has provided throughout my stay at Missouri S&T. I am thankful to Todd E. Sparks for his encouragement, advice and critiques on various aspects of work. I must also thank the Manufacturing Engineering department for the financial assistance provided during the pursuit of this research.

I would like to thank Dr. Joseph Newkirk for the close participation, advice and guidance that he has provided throughout this endeavor. I would also like to thank Dr. Edward C. Kinzel for his timely advice. I would like to thank Dr. Newkirk and Dr. Kinzel for being a part of my thesis committee.

I most sincerely thank the members of LAMP lab for making this journey an exciting and educational experience. I would especially like to thank Niroop Matta, Sai Aravind Palepu and Sriram Praneeth Isanaka for their assistance and constructive criticism at various stages of the study. I am also grateful for the support I received from all my friends at Rolla.

Finally, I would like to express my deep gratitude to my parents, Dr. Somaiah Karnati and Mrs. Shantha Devi Karnati, and my sister Priyanka Karnati for their unconditional love and support. Without their never-ending positivity and encouragement, I would not have been able to pursue my interests with such passion.

TABLE OF CONTENTS

LIST OF ILLUSTRATIONS

Page

LIST OF TABLES

Page

NOMENCLATURE

Symbol	Description
H.T.R	High Temperature Region
J.S.R	Just Solidified Region
M.Z	Mushy Zone

1. INTRODUCTION

1.1. BACKGROUND

Laser metal deposition (LMD) is an additive manufacturing technology, where a layer-by-layer build schema is used to the manufacture of complex geometries with excellent material properties. Unlike conventional manufacturing processes where a part of desired shape is machined from a blank work piece, LMD builds the required structure by systematically adding material to a substrate. In the case of metals, a high power laser is used to melt material in the form of powder or wire onto the substrate [1].

Real time control of process parameters is crucial and necessary to reliably achieve a repeatable and quality product from any production process. Similar control requirements are expected for Laser Metal Deposition (LMD) as it comes with its own set of complexities and attributes which could be addressed using closed loop control. The commercially available laser based additive manufacturing technologies such as LENS (Sandia National Labs), Direct Metal Deposition (UIUC) [1-5] etc. are incorporated with proprietary feedback systems set to monitor a characteristic attribute during deposition. However the robustness and sensitivity of the feedback control systems dictate the precision of control over the geometric tolerances, and mechanical properties that can be achieved using LMD.

Attempts for identifying qualitative and quantitative significance of process parameters exist in literature [6, 7]. Some of the research utilized analyses of the output generated by varying a multitude of process parameters to develop control schemas. For example, modulation of laser power during deposition has been reported as an effective method of achieving targeted properties, owing to the fact that the input power significantly affects output strength, microstructure, surface finish and tolerances of the fabricated part. Considering temperature to be the direct consequence of input power, acquisition of thermal history can thereby be crucial in training process control mechanisms and also learning the influence of, and the interaction between other process parameters.

From literature we understand that various strategies have been employed to develop control mechanisms for laser based manufacturing processes. The popular choice for the same has been statistical analyses and development of optimal parameter maps [10, 11]. Efforts have also been made to establish closed control loop control over many high temperature processes including laser melting, welding and Tungsten Inert Gas (TIG) welding processes. Sensors like Charge-Coupled Device (CCD) cameras, spectrometers, acoustic sensors and pyrometers were used to monitor meltpool size, surface and plasma variations to detect deviations and correct process parameters to maintain ideal deposition conditions [12-19]. These implementations of closed loop systems involved monitoring and/or controlling attributes such as temperature, color, size, volume etc. of the meltpool created during the course of melting or welding. The control mechanisms were then validated by the final product, but the author believes that little effort was extended towards decoupling the monitoring attributes to attain characteristic insight into the phase transformation phenomena.

Current research was initiated to decouple the monitored attribute and achieve a better understanding of the deposition and solidification processes. For the sake of brevity and clarity SS 304 was employed as the deposition material and an IR camera as the acquisition system wherein the IR camera's viability as a process monitoring tool was studied. Upon realizing its scope for capturing the deposition phenomenon, IR camera monitoring was determined to be a feasible acquisition method. The data acquired during deposition was then processed to locate and estimate the size of meltpool, mushy zone and solidus regions. The sensitivity of the processing methodology was put to test by analyzing a series of depositions performed with a multitude of process parameter variations and diverse substrate geometries. For the sake of simplification the work in the study was divided as follows,

- Vision based process monitoring for LMD processes
- Thermographic investigation of LMD
- Quantitative and qualitative analysis of the variables involved in the depositions

1.2. VISION-BASED PROCESS MONITORING FOR LASER METAL DEPOSITION PROCESSES

This portion of work was aimed at validating the functioning of closed loop control systems developed at LAMP lab. The deployed control systems were intended towards maintaining size of the meltpool and ensuring a consistent build height through the deposition. The primary point of investigation was the incorporation of an infrared camera for capturing the process of deposition and visualizing the feedback loops in action.

Contrary to popular belief, an infrared camera does not measure the temperature of the body in field of view, but instead records the radiation emitted off the body (within its spectrum of sensitivity) and calculates the temperature values based on its calibration. In other words the accuracy of the temperature readings obtained depends on the accuracy of the input parameter values provided for calibration. In this case the input parameter of most significance is the emissivity value, which varies for materials based on the spectral wavelength sampled and their thermal characteristics. The highly dynamic nature of LMD can make it exceedingly difficult for accurate temperature measurement. With assumptions that relax the temperature and spectral dependence of emissivity, the acquired data was processed for qualitative and quantitative insight.

The primary attribute monitored in this section of study was the high temperature region on the deposit. Employing a gray body temperature measurement (single emissivity value, less than 1) the temperature of the entire deposit was acquired. The region with temperature values between the highest temperature on the body and a 150 degrees less than the peak was called the high temperature region. The control of the feedback systems was realized by observing the variation in the high temperature region values (area measured as number of pixels).

1.3. THERMOGRAPHIC INVESTIGATION OF LASER METAL DEPOSITION

The acquisition capabilities of the IR camera were sufficient to capture the deposition phenomenon and its resolution was significant enough to recognize the effect of variation in measured process parameters. The next phase of the study involved the

decoupling of data acquired to estimate the area of the meltpool, freezing zone and solidus regions.

During phase transformation there is a significant change in emissivity values of a material. Using this variation in emissivity as the basis, a decoupling method was hypothesized. The solid to liquid transformation results in a decrease in emissivity values [21]. If this decrease in emissivity is unaccounted in Plank's equation, the calculated temperature for the meltpool is noticed to be less than the calculated temperature of the solidus. Though this is in direct contradiction to reality this signature behavior can be employed to identify the location of the different phases.

The mechanism of LMD makes the meltpool progress in the direction of deposition trailed by the solidification front. Therefore at any given instance if the direction of deposition and the location of the laser on the deposit is known, the positions of the meltpool and the solidification front can be approximately estimated. Physics indicates that there is going to be a depleting amount of liquid phase as we move from the meltpool towards the solidification front, by which we conclude that the emissivity will increase as me move from the meltpool to the solidification front. Consequently the measured temperature readings would also rise as we move along the meltpool towards the solidification front.

Targeting this transition, edge detection techniques from image processing methodologies were applied on the acquired IR thermographs. The transitions from solid to probable liquid phase region were then estimated and the calculated pixels corresponding to each phase were summed. The areas of interest in this situation were the mushy zone and the just solidified region. The mushy zone was expected to comprise the meltpool and the freezing range with emissivity values less than the solidus. The just solidified region includes the lower range of freezing zone (with almost solid emissivities), the material at solidus temperature and solid material below the peak solidus temperature by 150 degrees.

1.4. QUALITATIVE ANALYSIS OF DEPOSITIONS VARIED IN SUBSTRATE GEOMETRY AND INPUT POWER

The formulated decoupling technique was further investigated by analyzing a series of four layer deposits performed on substrates shaped as thin-wall structures. Laser metal deposition of thin-wall structures is a complicated procedure where the change in thermal resistance with regards to conduction during part built results in varying build rates across the different heights. Without either feedback control or prior power planning, uniform deposition will be difficult. To overcome these issues the analysis was performed on thin-wall shaped substrates. Assuming minimum variation during deposition, four layers with a layer height of 0.05 mm each were deposited on substrates of varying size and input power. During the experimentation the size of the substrates was varied by varying the track length, substrate thickness and thin-wall height.

The thermal history of the depositions was captured using an IR camera, and this thermal data was then processed and decoupled using the formulated technique. The areas of interest including the mushy zone and the just solidified regions were averaged and plotted. The trends in these areas during depositions were analyzed by performing a linear fit to the data. The sensitivity of the camera and the decoupling technique used towards the variation in substrate size and input power was determined. The signatures of laser during power down, the effect of increasing thermal resistances, and ascending input power etc. were also identified and addressed.

1.5. ASSUMPTIONS AND STATEMENTS

The assumptions laid on the current analyses are,

- Emissivity value is expected to not vary with temperature and acquisition wavelength
- Setup for front view perspective is absolutely normal hence shapes of the calculated regions of interest are not projections

Steps have been taken to justify the assumptions to the best possible. The current analyses concentrate on calculation and analyses of the following regions of interest,

- Freezing range: This is the material with temperatures varying between the solidus and liquidus temperature values of a material.
- High temperature region: If T_M is the peak measured temperature in a thermograph acquired during deposition. The material on the deposit with measured temperatures in range of 150 degrees below T_M and T_M is called the high temperature region
- Just solidified region: This is material with measured temperatures same as the high temperature region.
- Mushy zone: This is a calculated estimate obtained upon employing the thermograph decoupling methodology. The theorized constituents of this zone/region are the meltpool and most of the freezing range.

2. VISION BASED PROCESS MONITORING FOR LASER METAL DEPOSITION PROCESSES

2.1. INTRODUCTION

Free form fabrication of metal by direct metal deposition is an excellent method for fabrication of complex geometries and high precision repair. The term "Direct metal deposition" coined at University of Illinois Urbana-Champaign, is a technology where a high power laser is focused to melt a stream of injected powder to build parts in a layer-by-layer fashion. This process possesses the scope for great accuracy, controllable microstructures and the feasibility of manufacturing functionally graded materials [1]. Direct metal deposition technologies such as "Laser Engineered Net Shaping (LENS)" have been under development by Sandia National Labs with extensive university, industry and government participation [2-5]. In these methods of fabrication a laser melts the powder completely to form dense parts with small heat affected zones that result in fine microstructure and excellent material properties [6]. It is believed that the physical aspects of the parts made by the "Laser Metal Deposition (LMD)" or DMD processes such as strength, surface finish and tolerances are dependent on the thermal history of the process [7]. Monitoring the thermal history during deposition would therefore be instrumental in realizing various dynamics that occur during deposition and can thus provide basis and rationale for better process planning and even model validation.

In some cases existing technologies incorporate thermal acquisition systems for bettering the procedure of fabrication by additive processes. As an example thermal imaging systems have been integrated into the Selective Laser Sintering (SLS) process to monitor its thermal history, correlate the outcomes and help plan an optimized approach for part manufacture [7-9]. The highly variant dynamics of this fabrication procedure make temperature acquisition a complicated phenomenon. For a chosen approach of acquisition, the degree of accuracy of input parameters dictates the accuracy of the measured temperature.

There are large number of complexities that need to be addressed for temperature acquisition. In the current effort an IR camera has been chosen as the acquisition system.

Temperature acquisition using infrared thermography requires accurate input parameters to guarantee accurate outcomes. The most significant of these parameters are the emissivity, along with the high melting and cooling rates observed during deposition which complicates the acquisition setup. Phase transformations in the material during deposition, including melting and solidification result in the corresponding drop and rise of emissivity of the material being deposited. In the case of metals the shiny surface composition causes lower emissivities, but upon oxidation of the surface from laser interaction a significant change in emissivity occurs. Surface oxidation thereby results in variations in emissivity and distilling this down to a single value for emissivity during temperature evaluation would require significant post processing.

The topic of study for this endeavor was to realize the functioning of closed loop control systems employed on LMD systems at Laser Aided Manufacturing Processes (LAMP) lab. The chosen acquisition system was a FLIR A615 industrial automation infrared camera. A set of assumptions and evaluation criteria were developed to incorporate and establish the camera as a process monitoring tool. The need for post processing the thermal data was circumvented by assuming spectral and thermal independence of deposited material's emissivity. The deposition procedure was analyzed by monitoring the size of the high temperature region (H.T.R)

2.2. EXPERIMENTAL SETUP

The study involved monitoring LMD of a thin-wall structure by recording the thermal history during the deposition process using an infrared camera. The infrared camera used was manufactured by FLIR and has a maximum resolution of 640x480. The working spectral range of the camera is from 8µm to 14 µm. The acquisition sensors in the camera were micro-bolometers. The camera was placed at a distance of 0.4 m from the site of deposition, to record the thermal data during deposition in a front view perspective. The material of deposition was 304 Stainless Steel gas atomized powder acquired from Carpenter powder (-100 +325 mesh). The dimensions of the deposited thin-wall structure were 25 mm long and 25 mm high.

The deposition was performed using a 1kW Fiber laser with a wavelength of 1064nm, manufactured by IPG photonics. The spot size used to perform deposition was

approximately 1.5mm. The deposition system was a worktable custom built at LAMP lab with a resolution of 2 microns. The schematic view of the setup is as shown in Figure 2.1.

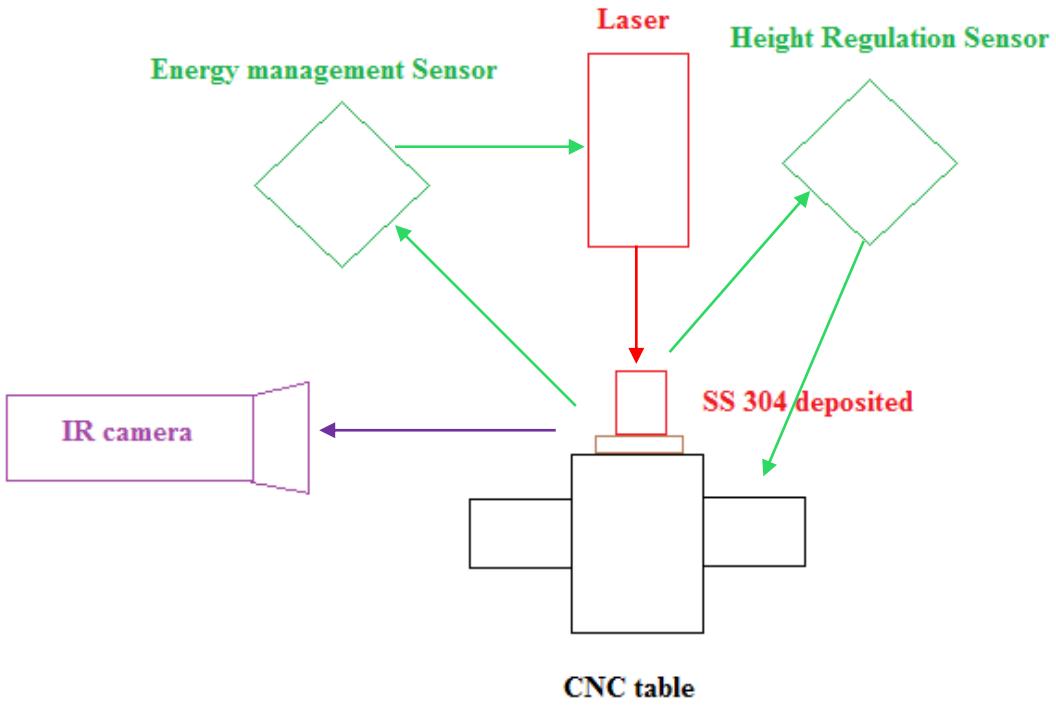

Figure 2.1. Schematic side view of the experimental setup (arrows indicate direction of data transfer)

The deposition system was equipped with two closed loop control feedback systems:

(a) The first aimed at maintaining the amount of energy (Energy Management System) in the deposit and

(b) The second to ensure a consistent build height (Height Regulation System) throughout the deposition.

Energy management system is an incorporated control system to ensure homogeneity in properties of the fabricated part. It ensures that all the layers are built

using a uniform energy input throughout part construction. This can be elaborated as establishing a steady state scenario along the size of the meltpool, material at freezing range temperatures and material around solidus temperatures (from here on referred as high temperature region) [7,8]. The schematic logic for this control system, is shown in Figure 2.2.

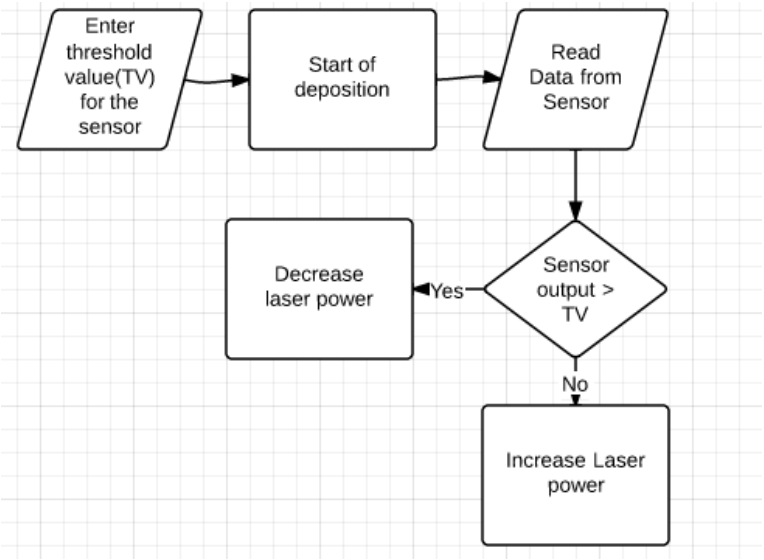

Figure 2.2. Flowchart logic for energy management system

The control system maintains the system parameter/sensor output (in relation to the size of the high temperature region) around a pre-determined threshold value (in Figure 2.3) by increasing or decreasing the input power as necessary. The higher the value of the threshold, larger is the allowable size of the high temperature region, which directly corresponds to the amount of input power.

Height Regulation System, is another control system that compensates for the build height inconsistencies that occur during deposition. It compensates for over or under building by rushing or slowing down the work table to increase or decrease the

material deposited at a site. This ensures a build with sizes in-line with the input dimensions. The schematic logic for this system is shown in Figure 2.3.

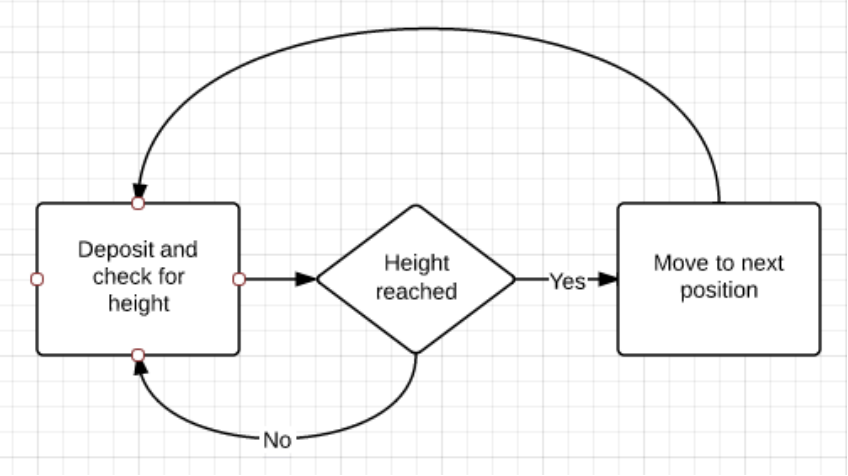

Figure 2.3. Flowchart logic for the height regulation system

The assessment of build height at each location was done by analyzing the height regulation system sensor value (in relation to height of solidified material). If excess material was deposited the work table swiftly moved to next location to minimize further accumulation of material. If the material deposited was lower than the required amount, the work table slowed down till it reached the required height and then moved onto to the next location continuing deposition. The energy management system compensates for the speeding up or slowing down of the work table by increasing and decreasing the input power values as necessary.

Thin-wall structures were deposited using the above setup and the IR camera was used to visualize the effect of these closed loop control systems on material deposition. Three threshold values with a qualitative significance of Low, Medium and High (in relation to input power) were used for the energy management system. Simultaneously powder feed rate was also varied as 10, 30 and 50 gm/min to see the effect it has on the height regulation system.

2.3. IR CAMERA INTEGRATION

An IR camera captures the radiation coming off a body and compares the gathered values against calibrated data from a black body to estimate temperature. If the supplied emissivity value was higher than the actual emissivity of the measured body the output temperature would be colder than its actual temperature. If the supplied emissivity was lower than the actual emissivity value, the measured output temperature value from the camera would be higher than the actual temperature. This behavior complicates temperature acquisition during LMD, since there is a phase transformation that occurs during deposition. Liquid metal has a significantly lower emissivity in comparison to solid metal (the reflective properties are better in liquid state as compared to solid). Therefore if the structure during deposition was to be studied with the solid body emissivity as the input value, the measured temperature (as measured by the camera) of the melt pool would be less than that of the solid region, which would contradict reality. If the pre-set emissivity value was equal to that of the melt-pool, we could obtain the correct range of measured temperature values for the melt-pool but, the solid portion temperatures would appear hotter than in reality. Therefore assumption and adaptation of a single emissivity perspective would be erroneous. Since most of the deposit was in solid state, the input emissivity value was chosen to be that of the solid.

The primary purpose of the investigation was to monitor the area of the high temperature region. As discussed in the previous sections, the accuracy of measured temperature values using an IR camera is highly dependent on the accuracy of the input parameters supplied. The parameter of most significance emissivity, which is dependent on spectral and temperature variations. For the current study the spectral dependence condition was relaxed, because the quantitative variation of the emissivity in relation to the spectrum sensitive to camera is an unknown. The emissivity value of metal oxides is significantly higher than their corresponding pure metal counterparts. Therefore to minimize the material variation on the surface, deposition was performed in an open atmosphere (open to air). The emissivity of the oxide scale for the current material under deposition (SS 304) was obtained by averaging the oxide emissivity values of the constituent elements in the alloy. Open atmosphere deposition resulted in consistent

surface oxidation, where the variation in emissivity with temperature was assumed to be minimal as the emissivity value was already close to 1 (0.9) at room temperature.

The above assumptions about emissivity and measured temperature values needed revision for the high temperature region. Since the chosen emissivity value was probably close to the solidus's actual value, the measured value of temperature at the hottest site should be around the solidus temperature of the material being deposited.

The analysis of the depositions was performed by measuring the area of the high temperature region. The possible constituents in this high temperature region would be the completely solid material (with temperatures in chosen range) and lower ends of freezing range where the presence of liquid phase made the material appear colder.

2.4. RESULTS

By simultaneously varying the threshold values for the energy management system and the powder feed rate for height regulation system, nine depositions of 25mm by 25mm thin-wall structures were recorded using the IR camera. For visualization, the temperature data was represented by an iron color palate to indicate the thermal profile of the deposit. An in-situ snapshot of the deposition is shown in Figure 2.4.

Figure 2.4. Rendered thermal image of deposit using an iron colored palate

The acquisition frequency of the camera during these depositions was 200 fps. The nine depositions performed by varying the threshold values and powder feed rates were thermally mapped using the camera and post processed to identify the high

temperature region. The temperature cutoff imposed was to list the area (number of pixels) that qualifies under the criterion. A snapshot of the deposition with iron color palate rendering after post processing is shown in Figure 2.5.

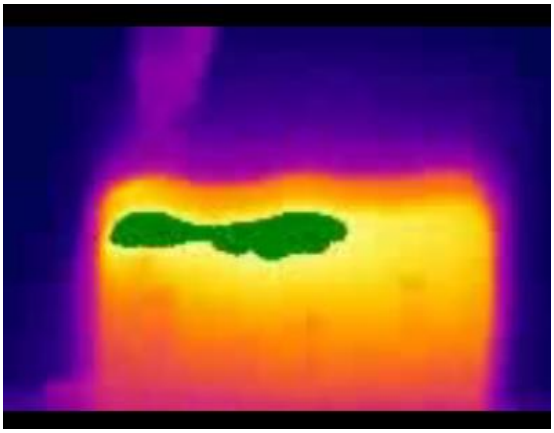

Figure 2.5. Green color depicts the high temperature region

The control of the energy management system was realized by logging power modulation during depositions. The plot in Figure 2.6 shows one of the consequent power outputs from using energy management system.

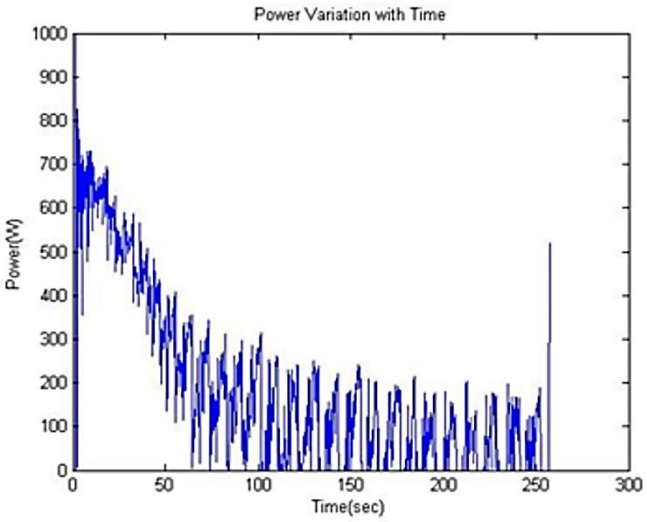

Figure 2.6. Power log depicting power modulation for a threshold value of 1(low)

The area of the high temperature region vs. time was plotted for the settings of 10, 30 and 50 gms/min powder feed rates at each of the threshold values. The obtained results are shown in Figures 2.7-2.9 as follows.

Figure 2.7 shows the variations in the area (number of pixels) of the high temperature region for depositions done with the energy management system set at a threshold value of 1 (low) for powder feed rates of 10, 30, and 50 gms/min respectively. It can be noticed from Figure 2.7 that the time taken to complete the deposit was different for each powder feed rate. Similar attributes have been seen in the plots made for depositions done at the threshold value 2 (medium) and the threshold value 3 (high) with different powder feed rates (shown in Figures 2.8 and 2.9).

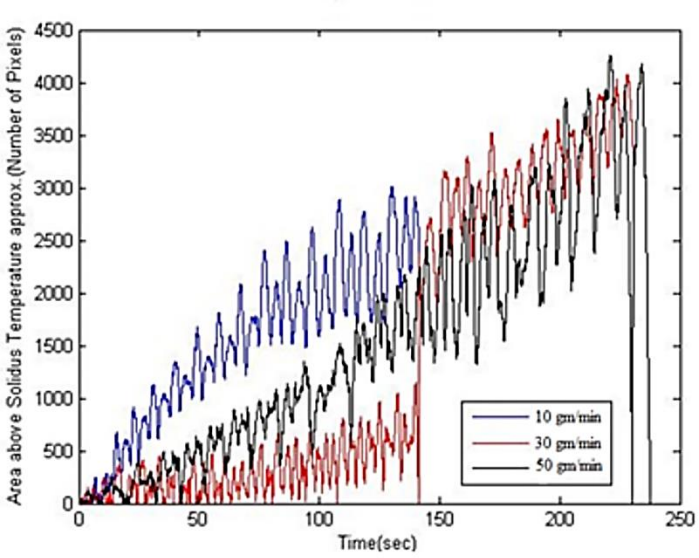

Figure 2.7. Area of the high temperature region for a threshold value of 1(low)

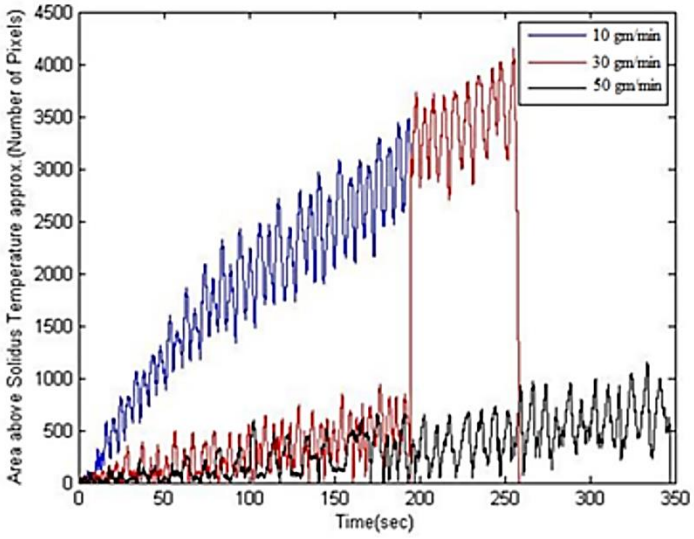

Figure 2.8. Area of high temperature region for the threshold value of 2 (medium)

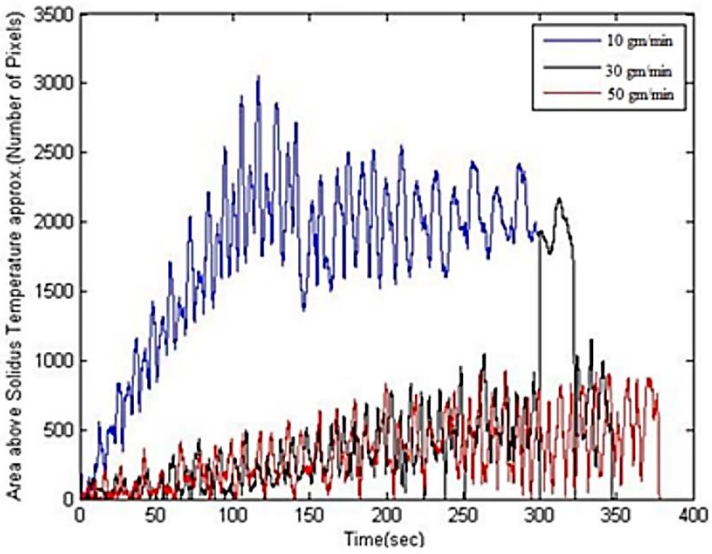

Figure 2.9. Area of high temperature region for the threshold value of 3 (high)

2.5. DISCUSSION

The current monitoring efforts were based on the temperature readings gathered from the IR camera. The melting and solidification and resulting liquid and solid phases exhibit different emissivities. These emissivities result in the camera reading a multitude of temperatures. The spectral and temperature dependence of emissivity further complicates the accuracy of temperature acquisition. For the current study corrections for spectral and temperature dependence have not been implemented. Thus the analysis was limited to a qualitative estimate used only for capturing the functioning of the feedback systems.

The logged values of power indicate the variation of power with respect to time caused by the feedback system (Figure 2.6). The high temperature region of the deposit was identified by imposing the temperature criteria on the acquired thermal data and was represented in green, as shown in Figure 2.10.

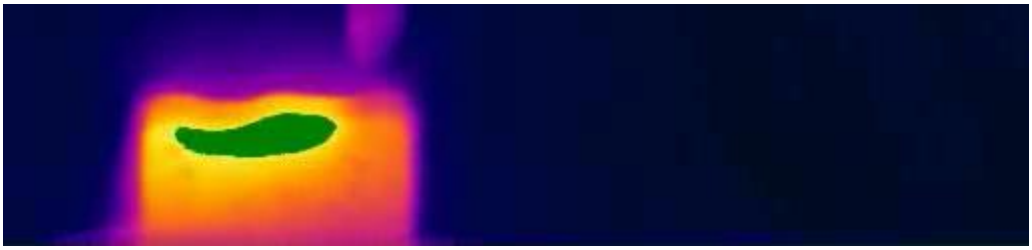

Figure 2.10. Green color depicts the high temperature region

The logged values of power (Figure 2.6) indicate a decay in the median value of power during deposition. This could be described as the energy management system varying power to initiate and control deposition. After a steady state scenario was sensed an almost constant median power to maintain this steady state was detected. The value of power stays high during the initial stages to heat the substrate and then stabilizes after the establishment of the steady state. The dips in the power graphs are expected to match the geometric end points of the thin-wall structure, where the laser is shut off between subsequent layers. The control of the energy management system and effect of power modulations can be better seen from the plots of the area of the high temperature vs time. In all the cases there is a rise in the area of the high temperature region which is followed by the median stabilizing. The rises and dips are theorized to be the consequences of the laser powering off and on between layers.

Trends in area of high temperature regions also highlight the operation of the height regulation system. If the systems sensed a discrepancy in the height deposited, the work table was to be slowed to compensate for the lagging height. As the machine slowed down more amount of heat was input into the deposit and the area of the high temperature region thereby increased. After the deposited height reached the sensor's requirement the work table sped up and energy management system established a steady state again. This behavior can be seen Figure 2.7 (red), Figure 2.8 (red) and Figure 2.9 (black).

The results from this analysis could also be interpreted to estimate optimal work parameters. It is believed that excellent mechanical properties can be achieved by creating smaller heat signatures during deposition, and with the use of a control system a

reliable and repeatable output can be established. The deposition time and trends in the area of the high temperature region can be used to identify the ideal parameters based on the thermal attributes during deposition. From the above analysis it can be concluded that

- Higher area of high temperature region could imply surplus amount of heat input and result in higher median temperatures during deposition.
- Having longer periods of deposition could imply larger wastages of powder, since the deposition doesn't operate at a hundred percent efficiency.

2.6. CONCLUSIONS

In the current topic of study a FLIR industrial automation camera was incorporated as a process monitoring tool to study the functioning of closed loop control systems developed at the LAMP lab. Acquisition through an IR camera was established as a viable approach and, a methodology was laid out for qualitative analysis of the thermographic data acquired from the IR camera. A temperature based criterion was established to identify H.T.R, where the identified size of this region was treated as the signature attribute of the deposition. The trends in input power and the variation in the area of H.T.R were analyzed to identify and realize the working of the employed control systems. The control of the energy management system was clearly noticed through the stabilization in mean area value of the H.T.R. The sudden rise in the area of H.T.R was conceived to be the consequence of the control executed by the height regulation system. The observed variations in the area of H.T.R were in-line with the intended outputs expected from the control systems.

3. THERMOGRAPHIC INVESTIGATION OF LASER METAL DEPOSITION

3.1. INTRODUCTION

Song, Singh et al. [12] have incorporated a system of three CCD cameras and a pyrometer to track in real time and control the height and adjust the temperature of the melt-pool on a laser based metal deposition system. Control was achieved by monitoring temperature at the site of deposition and modulating the power. Similar process monitoring strategies have been studied for real time correction in plasma welding and laser welding. The attributes such as weld pool diameter, surface of the weld pool, and the weld plume size etc. have been captured and in some cases real time correction schema were established for the same. Kovacevic et al. [13] incorporated a CCD camera and illuminated the weld pool with a laser to capture the surface detail and there by perform a real time correction of the process. The camera was set to only capture the irradiating laser light and record surface detail. By modulating arc current, shield gas rate, and scan speed etc. the required control was executed. Zhang et al. [14] while performing laser lap welding have used a spectrometer to analyze the plasma formed during welding to monitor the process and used a co-axially set up CCD camera to capture the weld pool. The intensity of characteristic peaks in the plasma were monitored to realize the ongoing dynamics of the welding process. Also by incorporating image processing and edge detection techniques they have been able to identify defects occurring during the process. Huang et al. [15] using an infra-red camera have acquired temperature data and performed interference analysis on their hybrid laser and TIG welding system to track the seam during welding. Similar attempts were performed using acoustic sensors, CCD cameras, and pyrometers etc. to monitor the process and extract key attributes using image processing or other calibrated setups [16-19].

The above discussed monitoring efforts were focused on observing a signature attribute such as temperature, size or weld plume etc. and a data base of rules was established through decision-based iterative experimentation. Less effort was put to decoupling the monitored data and realize solidification. The models and control schemas were validated by simply monitoring the final output from fabrication. In this effort

though, a processing methodology for obtaining representative insight into the process of solidification was developed. The captured thermographic data was processed by imposing a temperature based criterion to identify the Just Solidified Region (J.S.R) and also estimate the location and size of Mushy Zone (M.Z). The M.Z during deposition was identified by processing the temperature data using edge detection methodologies from image processing techniques. The processed data is theorized to contain vital knowledge of the solidification of material. The decoupling of the deposition region would in future lay basis for an extensive study of the process.

3.2. EXPERIMENTAL SETUP & BACKGROUND

Laser metal deposition being a dynamic process with vast temperature differences across the deposit would require parameter values which vary significantly and irregularly along the body. The most pertinent and significant of them being emissivity, whose accurate measurement require that the spectral and thermal dependencies of the emissivity be identified and accounted for. For the initial set of experiments the thermal and spectral dependencies were assumed to be negligent. The thermal data studied in the previous chapter was considered for the development of the current technique. The capabilities of the IR camera are listed in Table 3.1. The schematic setup of the deposition system is shown in Figure 3.1.

Table 3.1. Specifications of the IR camera

Feature	**Specification**
Spatial resolution	0.69 mrad
Focal Length	25.4 mm
F-number	1
Imaging frequency	12.5 Hz to 200 Hz
Image resolution	640x480, windowing at high freq.
Temperature measured	3 ranges, -50 C to 2000 C (e=1)
Detector	Uncooled bolometer
Detector time constant	8 ms (typical)
Spectrum sensitivity	7.5 to 13 micron

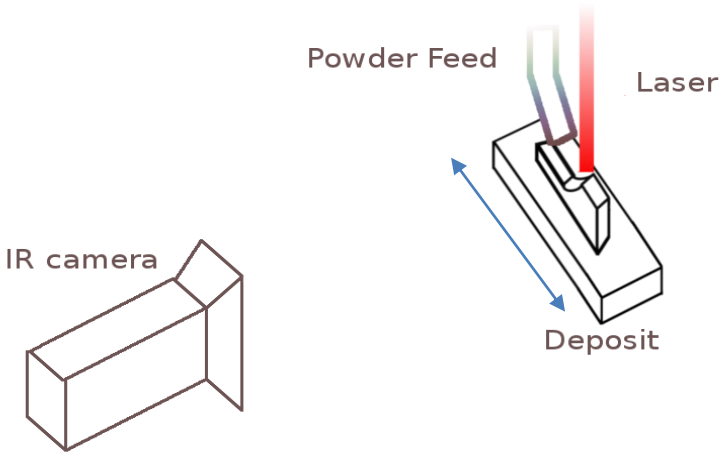

Figure 3.1. Schematic diagram showing the setup of the camera with respect to the deposit

The camera performs only a single gray body measurement which means that the acquired temperature data would be obtained with a single emissivity. Literature review states that the emissivity of metal oxide (approx. 0.9 for SS 304 oxide) is higher than the respective metal (SS 304 metal, 0.3-0.4) and the emissive properties were favored by higher temperatures for the solid phase [21]. Therefore to rationalize the single gray body measurement the deposition and acquisition were performed in open atmosphere, where the resulting surface had consistent oxidation.

3.3. IMAGE PROCESSING & RESULTS

From the analysis it can be seen that the emissivity of the solid phase (oxide formed on SS 304 during fabrication in open atmosphere) is higher than the emissivity of the liquid phase. Also, the radiation captured by the camera from the solid phase would be greater compared to the liquid phase. Table 3.2 lists the calculated band radiance from solidus and liquidus phases for SS 304 in the camera's spectrum. Since SS 304 is not a eutectic composition and also has a freezing range, its fuzzy boundary can be expected between completely liquidus phase and completely solidus phase. This transition is expected to result in a drop in emissivity across the solidus to liquidus boundary and rise in the opposite direction. Figure 3.2 shows a schematic representation of the boundaries formed during deposition.

Table 3.2. Band radiance of solid and liquid phases of SS 316

SS 304		
Temperature	Emissivity [12]	Band radiance (7.5 to 13 micron)
Liquidus, 1400 C	0.3	4745 W/sq.m/sr
Solidus, 1377 C (oxidized)	0.95	1582 W/sq.m/sr

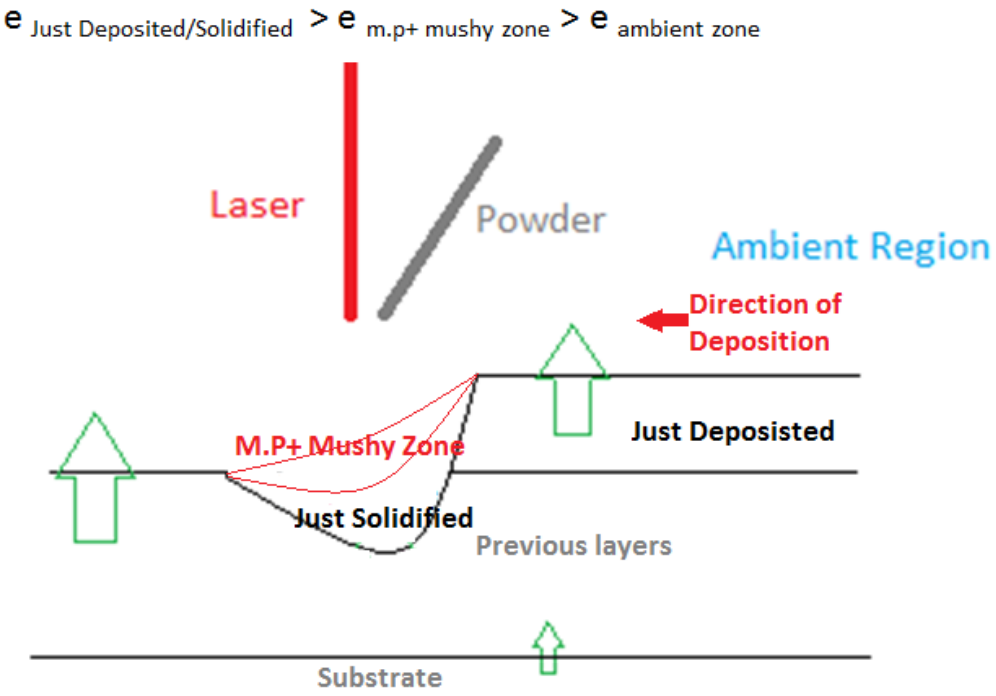

Figure 3.2. The boundaries and emissivity change trends in a thin-wall during deposition

The band radiance values in Table 3.2 indicate the reason for measured temperature values of liquid phase being lower than that of solid. When the liquidus band radiance signal was processed to evaluate temperature in the case where the correct emissivity value was not provided, the liquid temperature would appear lower than the temperature of the solid.

Boundaries in Figure 3.2 indicate the probable drops/rises in temperature caused by difference in emissivity values or the orientation. The characteristic regions identified in this study were named as the just solidified region, the mushy zone and the melt-pool. The probable constituents in J.S.R were expected to be completely solid material within the imposed temperature criterion and material at the lower end of freezing range temperatures. The presence of lower end of freezing range was also expected due to the lower emissivity values resulting from the presence of a liquid phase. It was expected that a significant drop in emissivity would occur when travelling from 100 percent solidus to

100 percent liquidus material. This drop was expected to occur within the freezing range of the material being deposited. Distinguishing between the higher end of freezing range and the melt pool was expected to be impossible. Since the imposed assumptions of temperature independence meant that the completely liquid phase and higher ends of freezing range (with regard to temperature) would exhibit similar emissivity values. The presence of these transitions was first realized by performing a discrete thermal gradient analysis across the horizontal and vertical directions of the thermograph. The variation in temperature across both was expected to bear a correspondence to the transitions in the material's emissivity values. The evaluated vertical and horizontal gradients of temperatures (a snapshot) during deposition are shown in Figures 3.3 and 3.4.

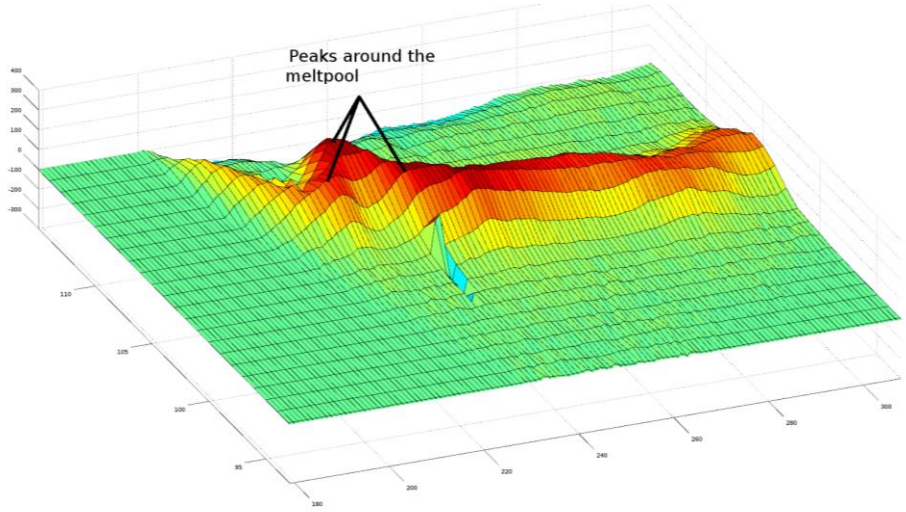

Figure 3.3. Peaks occurring around the deposition and the top edge of the deposit when the temperature gradient was plotted along the vertical direction

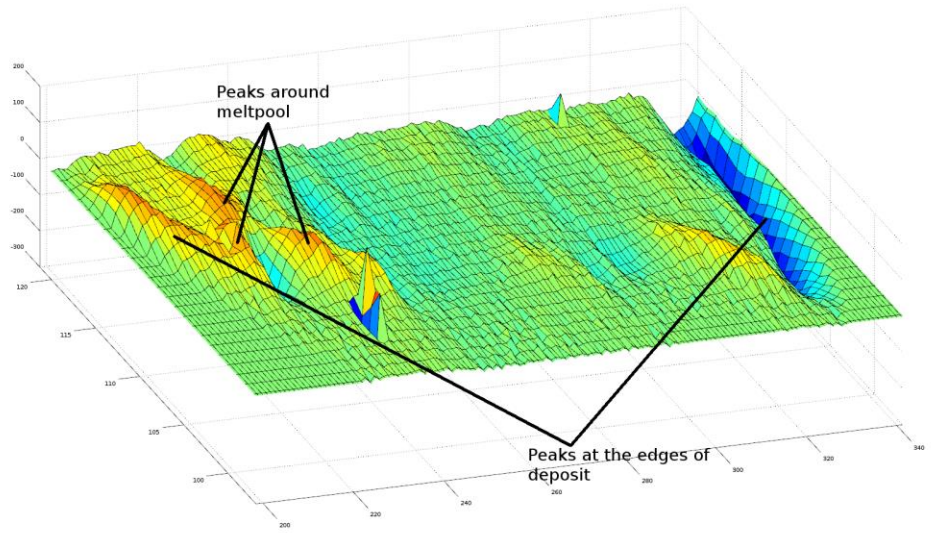

Figure 3.4. Peaks occurring at the vertical edges and surrounding the deposition region after the temperature gradient was plotted along horizontal direction

Figure 3.3 indicates peaks in the vertical gradient of temperature values, and these peaks were theorized to result from the rise in temperature in the solid region close to the melt-pool, (possibly in the freezing range caused by the dip in emissivity and the top boundary of the deposit). The peaks in Figure 3.4 indicate the rise and drop in temperatures obtained by performing a horizontal thermal gradient study. The peaks were expected from the side boundaries of the deposit and M.Z to the J.S.R and J.S.R to M.Z transitions.

In image processing studies, a variation in color/signal resulting from differences in material, orientation, lighting conditions etc. is referred to as an edge. The edge is identified by the characteristic drop/rise in the signal being studied. The sudden drop or rise in temperature while moving across the mushy zone and just solidified zone were treated as an edge in this study. Laplace edge detection was chosen to identify the transitions in the deposit. The algorithm of the employed edge detection technique is shown in Figure 3.5.

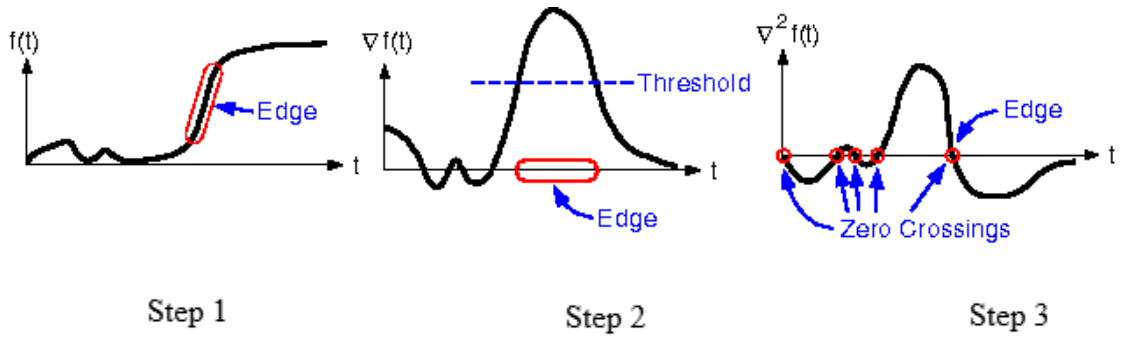

Figure 3.5. The steps in Laplace edge detection [22]

If f(t) was the signal under study in the t-parametric space, the rise in the value of f(t) is considered to be an edge. If a single and double discrete derivate of f(t) were evaluated, it can be noticed that a peak occurs in the single discrete derivative and a zero crossing occurs in the double discrete derivate at the site of the edge. An edge can be identified from a single discrete derivate value but a precise estimate can be derived from the double discrete derivative since a zero crossing is expected at the edge. The required transitions can be identified by imposing a threshold criterion to dispose edges resulting from minor variations or noise generated during acquisition.

Image processing and edge detection techniques were implemented on the captured thermographs using Python libraries [23]. The intended transitions were captured after a series of smoothing, gradient and edge detection operations. The detailed implementation of image processing techniques and step wise outputs (iron color palette rendered thermograph images) are listed below.

Moving median

Figure 3.6 shows the output generated after the implementation of a moving median filter. Moving median was applied by picking the median temperature value at every pixel from a series of 5 consecutive frames in the gathered thermographic data. Moving median operation was expected to remove powder particles, oxidation flashes and Johnson noise.

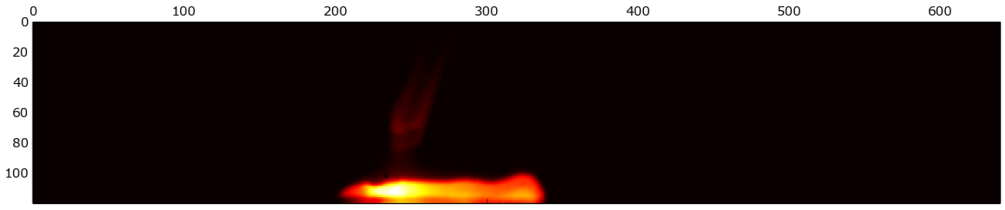

Figure 3.6. Rendered thermograph after a moving median filter implementation

Gaussian blur and Laplacian transform

While the moving median filter performed a temporal smoothing operation, this step was performed to carry out a spatial smoothing operation followed by a double discrete derivate. A combination function for Gaussian blur and discrete Laplace transform was implemented to achieve spatial smoothing and the double discrete derivative. The output image is shown in Figure 3.7. This data was referred as LoG (Laplacian of Gaussian). LoG was further processed to identify the zero crossings and estimate edges.

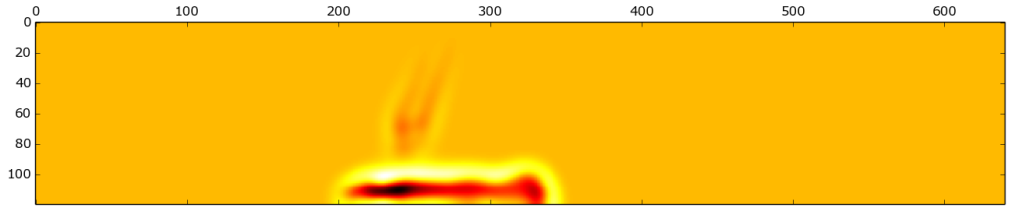

Figure 3.7. Output image from applying Gaussian and Laplacian transforms (LoG)

Zero Crossings

When the LoG data was scanned for identifying the zero crossings, a threshold was set to eliminate minor transitions and capture only significant transitions. The sites of the zero crossings were represented on a binary image (the sites of zero crossing were set as 1, the other pixels were set to zero). Figure 3.8 shows the sites of zero crossings obtained from the LoG data. The noticed boundaries are expected to be of the deposit and powder feed tube. The captured deposit boundary in Figure 3.8 includes the deposit shape without any included phase boundaries. The absence of edges from the M.Z to J.S.R can be attributed to the scale of the drop/rise (depending on direction of analysis) in temperature across the solidus-liquidus boundary being less substantial than the solidus/liquidus- air boundary.

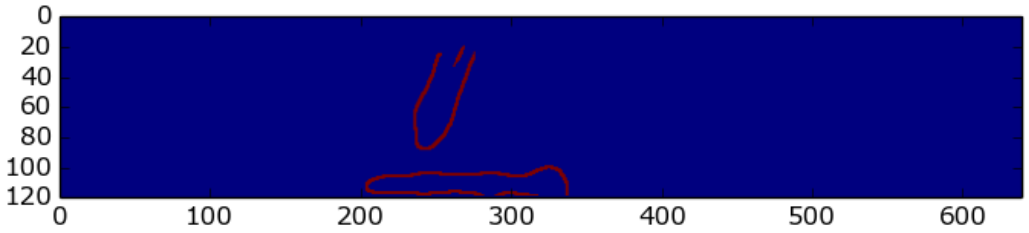

Figure 3.8. Sites zero crossings (red)

A further search for zero crossings within the deposit boundary was later performed to identify the mushy zone to just solidified region boundary. The powder feed tube was deleted from the binary image and the search was performed on a selected region within the evaluated deposit boundary. The region for the search was obtained by finding the area between the top boundary of the deposit and the top boundary of the just solidified region. Figure 3.9 shows the top boundaries of the deposit and just solidified region.

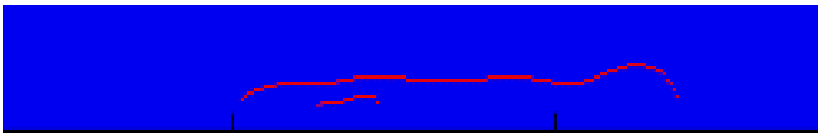

Figure 3.9. The top edge of the deposit and the top edge of solidus region

A search for zero crossings with a lower threshold was performed in the region between the top edges of the deposit and just solidified region. The transition between the mushy zone to just solidified zone was captured. Figure 3.10 shows the mushy zone, just solidified region and deposit boundary.

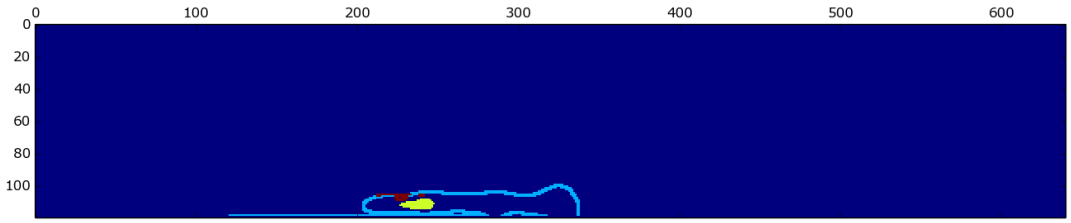

Figure 3.10. The mushy zone (red) and just solidified region (yellow) boundary of the deposit (sky blue)

Implementing the above steps of processing during various instances of the deposition (which were gathered using the control systems at LAMP lab) led to the generation of data which are visualized in Figure 3.11 for better understanding.

Figure 3.11. Mushy zone (white) just solidified region (yellow) and deposit boundary (red), left to right progression in deposition

Figure 3.11 shows snapshots from the deposition where the first layer of the deposit was being deposited. As the material deposited increases the conduction increases and the area of the just solidified region decreases in size. This can be attributed to the increase in thermal mass.

The Figures 3.12 (a) & (b) are snapshots from deposition indicating probable steady state. The size of the mushy zone and the just solidified region remained almost constant. Another point noticed was that the size of mushy zone increased with increasing deposited height, which can be explained by the increasing thermal resistance which is a consequence of the thin wall geometry.

3.12.(a).

3.12.(b).

Figure 3.12. (a) & (b). After steady state was achieved by the control system, left to right progression in deposition

3.4. CONCLUSIONS

An infrared camera was successfully incorporated as a process monitoring tool to identify the just solidified region and mushy zone during deposition. The thermal history of a 304 SS deposition was acquired and processed. Using a single gray body emissivity perspective and edge detection techniques the temperature data was filtered and processed. The deposit edges and the transitions between the liquid and solid phases were estimated successfully. The regions of interest were marked and snapshots from deposition performed with closed loop control were discussed. The insights gathered from this analysis were aligned with the basic dynamics of LMD.

4. QUALITATIVE ANALYSIS OF DEPOSITIONS VARIED IN SUBSTRATE GEOMETRY AND INPUT POWER

4.1. INTRODUCTION

In previous chapters an IR camera was incorporated as a process monitoring tool to monitor high temperature region during deposition. A post processing methodology was also developed to process temperature data gathered from the IR camera during deposition and estimate locations and sizes of mushy zone and just solidified region. The body of work involves performing a sensitivity analysis on the developed technique. The important parameters were dimensions of thin-wall structure and input power.

Construction of a thin-wall structure is a complicated process, wherein depositing at a uniform build rate with homogenous output would need closed loop control with constant monitoring. The controlled manipulation of the parameters would complicate the sensitivity analysis. The current effort was carried out on substrates with thin-wall shaped geometries. The dimensions were chosen to emulate the process of thin-wall construction. For a chosen track length the thin-wall section height was gradually increased to study the various stages of thin-wall construction.

4.2. EXPERIMENTAL SETUP

A fresh set of deposition experiments were performed using 1kW IPG photonics fiber laser with a focusing optics of 250mm, a beam diameter of approx. 2 mm, and an in house built powder feeder. The powder used for the deposition namely SS 304 was purchased from Hoganas with a particle size distribution of -100 and +325 mesh.

Experimentation was performed on substrates machined to mimic thin-walls. The substrates were all machined from a single block of SS 304 to maintain uniformity. The experiments were planned in order to capture effect of geometry and power. The experiments were all replicated twice, with the aim of confirming the repeatability of the analyzing methodology.

The geometry of the substrates was varied by varying the base thickness and the thin-wall height (Figure 4.1).

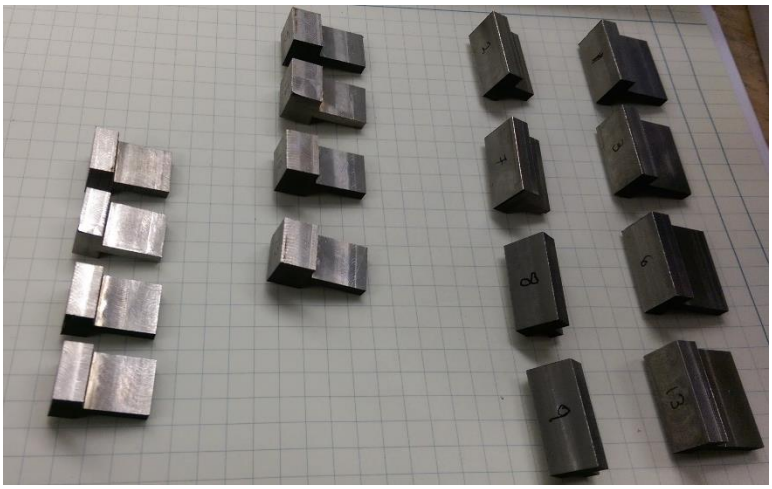

Figure 4.1. Substrate samples machined to mimic thin-wall

The variations in substrate geometry are listed in Table 4.1.

Table 4.1. The dimensions and names of the sample geometry

S. No	Base thickness	Track length	Thin-wall height	Sample name
1	6.3mm	27mm	6mm	Small
2	6.3mm	27mm	12mm	Medium
3	6.3mm	27mm	24mm	Tall
4	6.3mm	13.5mm	20mm	Short

Deposition procedure involved four layers at 250mm/min scan speed and 128 arbitrary units (roughly 15 gms/min) of powder feed rate on each of the sample substrates. The details of the conducted experiments were as listed in Table 4.2.

Table 4.2. Experiment details

S. No	Sample name	Power	Repetitions
1	Tall	750 W	2
2	Medium	750 W	2
3	Small	750 W	2
4	Tall	1000 W	2
5	Short	750 W	2
6	Short	1000 W	2

The acquisition was carried out at a capture rate of 100 Hz with an output resolution of 640x 240 pixels. In order to process accurate thermal data a single point dual color pyrometer was setup to acquire temperature for emissivity evaluation. The setup is as shown in the Figure 4.2.

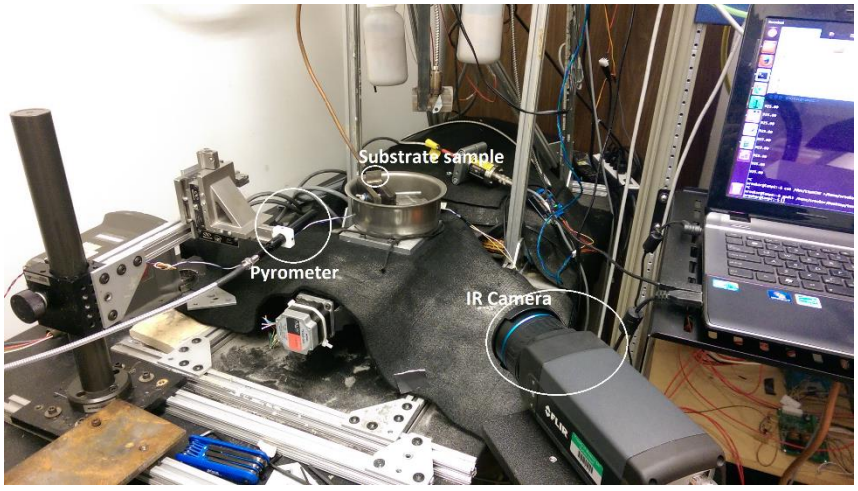

Figure 4.2. The experimental setup

The sample was setup at a 45 degree inclination w.r.t pyrometer and subsequently the IR camera was positioned to visualize the substrate in a front view perspective. The pyrometer view point could be identified using its guide beam, as shown in the closer look of the setup (as in Figure 4.3).

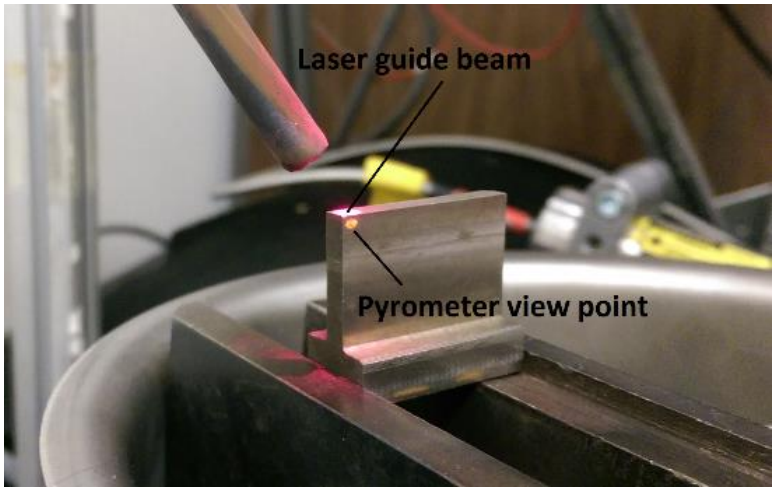

Figure 4.3. Pyrometer view point (orange) Laser spot (red)

4.3. RESULTS & DISCUSSIONS

The mushy zone is the region containing melt-pool and material at temperatures comprising most of the freezing range. The just solidified region is the region containing material at the lower ends of freezing range temperatures along with the material at and less than solidus temperature. The thermal data of the four layers of deposition from each experiment was analyzed to evaluate and locate pixel locations corresponding to mushy zone and just solidified regions. The temperature data was collected with the IR camera parameters set in Table 4.3.

Table 4.3.Parameters for the IR camera

Parameter	Value
Emissivity	0.6
Reflection Temperature	29 degrees Celsius
Ambient Temperature	25 degrees Celsius
External Optics Temperature	25 degrees Celsius
Optics Transmission	0.95

4.3.1. Image Processing. Exploiting the emissivity drop that occurs when solid phase transforms to liquid phase the drop/hike in temperature was identified using edge detection methodologies. The implementation of edge detection on IR thermographs was as represented in Figure 4.4.

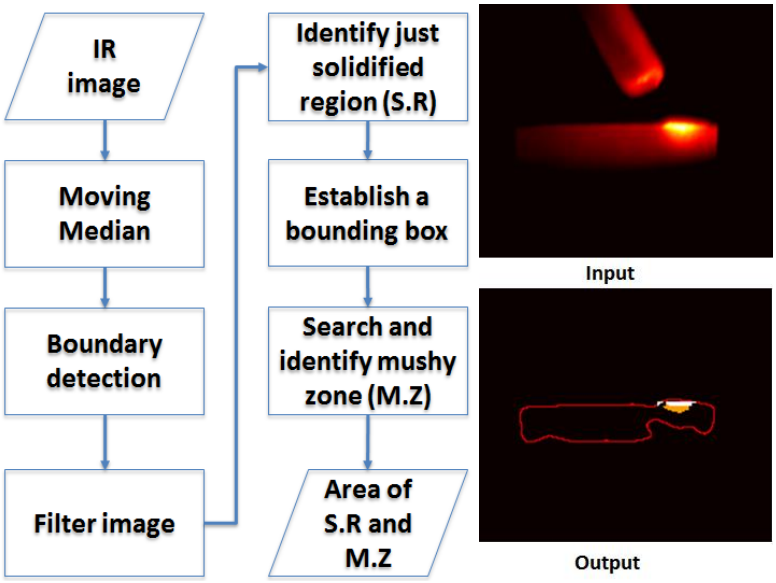

Figure 4.4. Flowchart of implementation of image processing, input and output

Through the depositions the number of pixels corresponding to mushy zone and just solidified region were noted and plotted as shown in Figure 4.5.

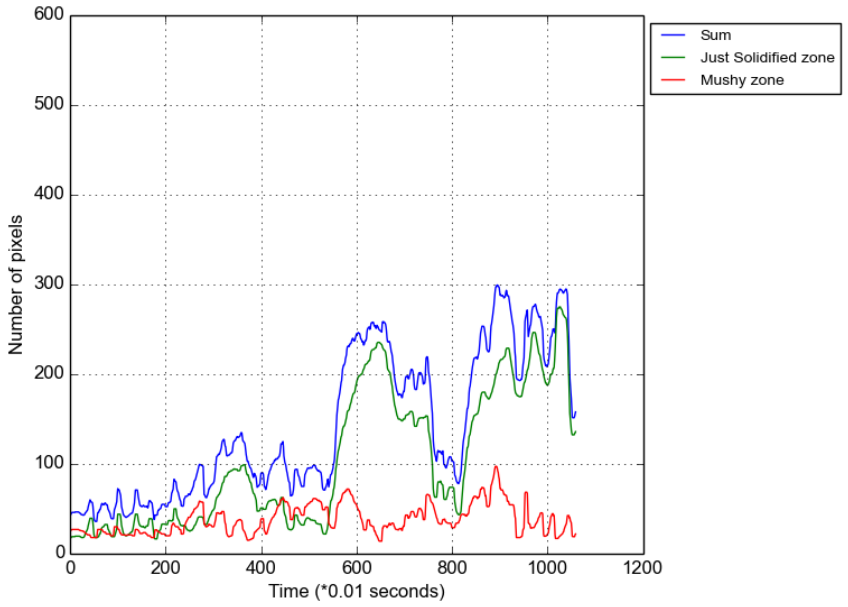

Figure 4.5. Output plot showing variation in number of pixels corresponding to mushy and just solidified zones

4.3.2. Varying Thin-wall Height. At a constant power of 750W four layers were deposited on the thin-wall substrates and the regions of interest (in pixels) were tracked. The output from the analysis for the three samples is shown in Figure 4.6.

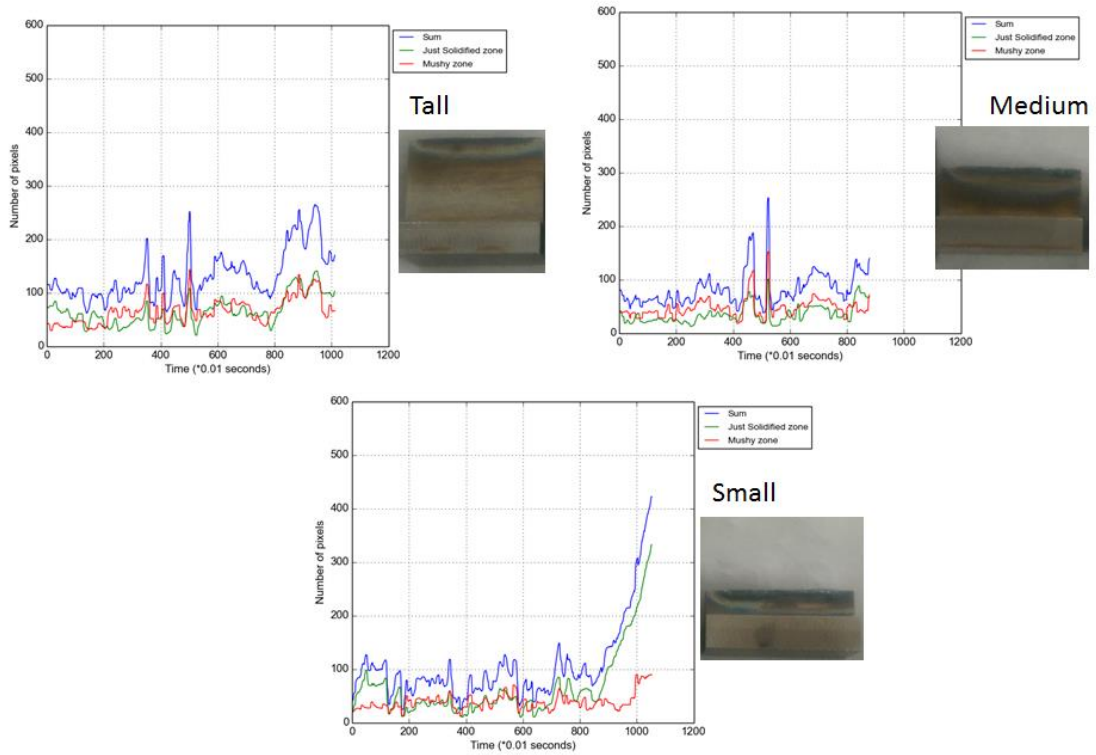

Figure 4.6. The area of r.o.is with varying height

Qualitative analysis was performed by fitting a linear polynomial (trendline) to the area data and compared to the increasing trend of each region with varying heights. The effect of height was identified by comparing the slope and intercept of these trend lines. The area and trend line plots for just solidified and mushy zone of a tall sample (height value) are shown Figure 4.7 and Figure 4.8, respectively.

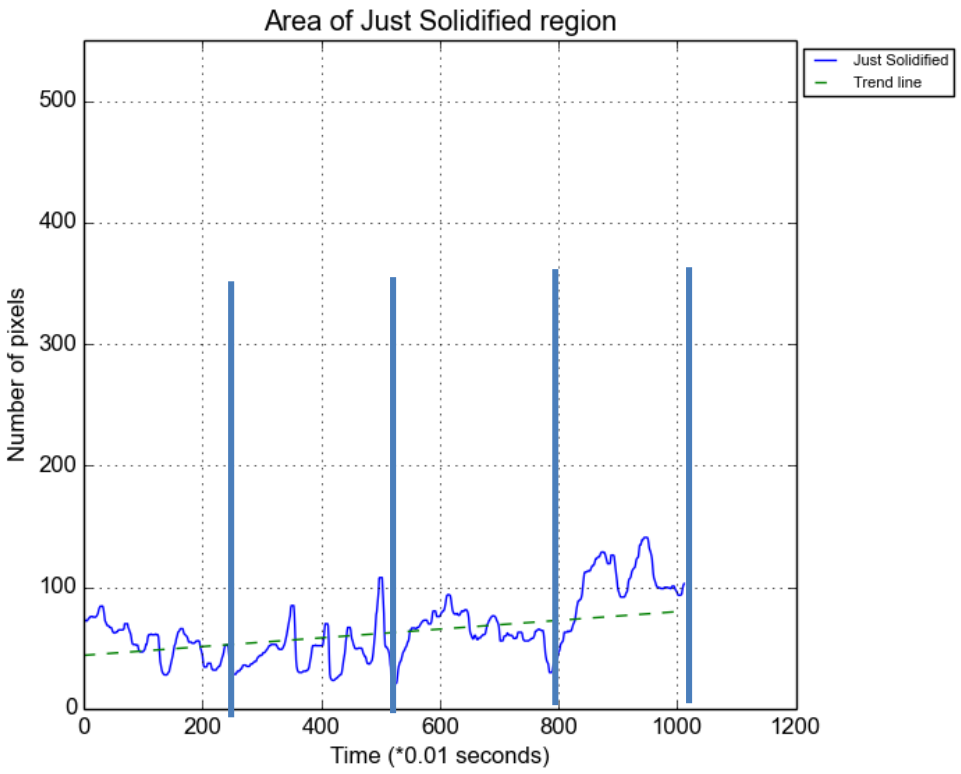

Figure 4.7 Area and trend-line of just solidified region during deposition on a tall sample

The blue lines in Figures 4.7 and 4.8 indicate instances where the laser was switched off and the deposition direction was reversed. The slope and intercept values of the trend lines plotted for small, medium and tall samples are shown in Tables 4.4 and 4.5.

Table 4.4. Slope and intercept values of trendline for area of mushy zone

Sample	Slope	Intercept
Tall	0.05	39
Medium	0.02	38
Small	0.02	28

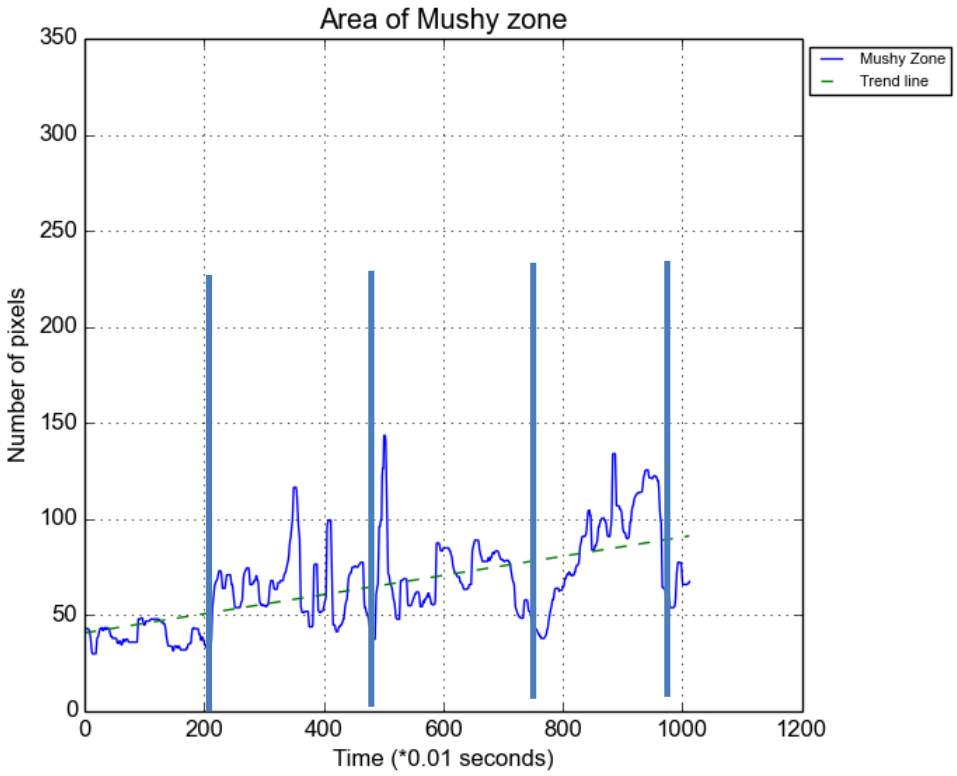

Figure 4.8. Area and trend-line of mushy zone during deposition on a tall sample

Table 4.5. Slope and Intercept values of trendline for area of just solidified zone

Sample	Slope	Intercept
Tall	0.04	43
Medium	0.03	22
Small	0.02	36

The values of slope suggest that there is a consequence to the varying heights of the thin-walls. In samples with taller sections there is a steeper ascension in areas corresponding to the mushy zone and the just solidified zone. This is synchronous with the fact that as the height increases the conduction path between the sink (substrate) and as the hot spot increases the thermal resistance also increases. This increases the amount

of heat retained in the deposit during deposition. The intercept values however, fail to give conclusive data, but were able to measure the starting point for mushy zone region to around 40 pixels in both cases.

4.3.3. Varying Power. On tall substrate samples, four layers of deposition with power settings of 750 W and 1000 W were performed. The regions of mushy zone and just solidified zones were tracked through the deposition and the corresponding output was plotted for comparison. A trend line was fitted for the mushy zone and just solidified zones for both powers and a slope intercept comparison was performed. The area outputs for 750 W and 1000 W are shown in Figure 4.9 and Figure 4.10, respectively.

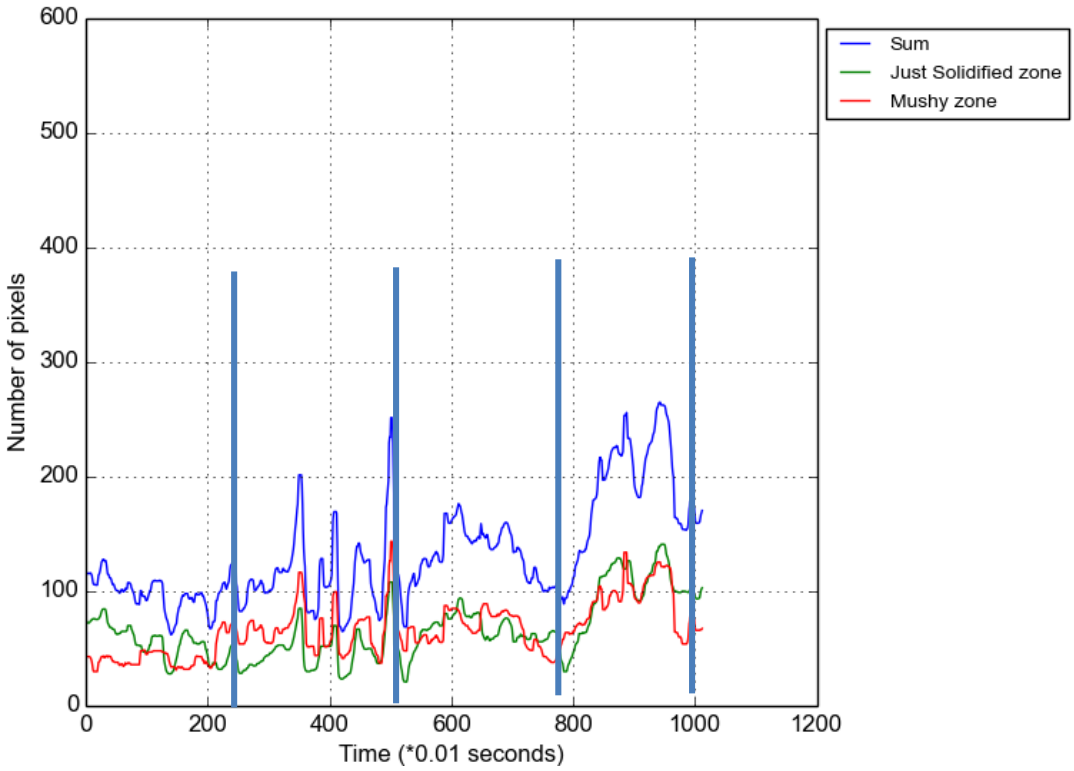

Figure 4.9. Areas of regions of interest for 750 W deposition

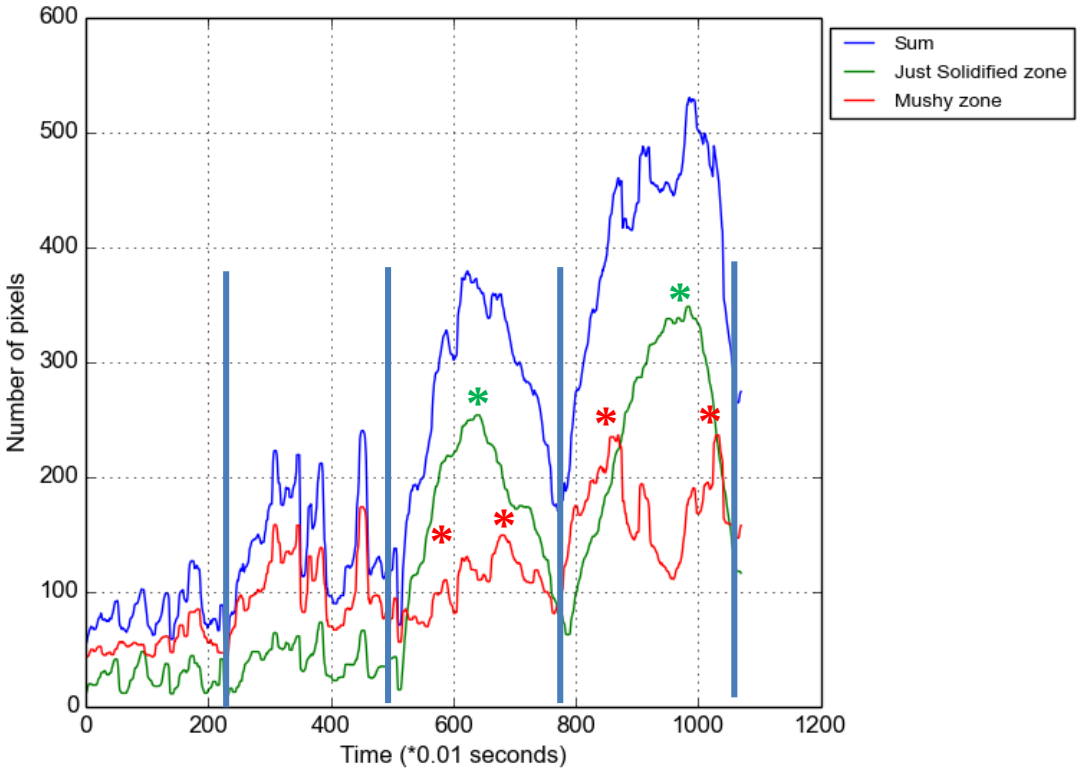

Figure 4.10. Areas of regions of interest for 1000 W deposition (Stars indicate peaks due to geometry of deposition)

The blue lines indicate the locations where the laser was turned off and the direction of deposition was reversed. The red asterisk (*) indicates rise and fall of the mushy zone and green asterisk (*) indicates the rise and fall of the just solidified region (Figure 4.10). The point to be noted is that the rise in mushy area happens when the deposition is in close proximity to the end points and as the laser approaches the central section of the deposit there is a dip in the mushy zone area and rise in just solidified area. This can be attributed to the fact that conductivity at free edges is low in comparison to locations inside the body. The prominent modes of heat loss are conduction and convection. The possibility for convection remains almost same whereas the medium for conduction drastically changes across the length of the thinwall.

The slope and intercept values upon performing a trendline fit to 750 W and 1000 W depositions are as detailed in Tables 4.6 and 4.7

Table 4.6. Slope and intercept values from trendline fit for just solidified region areas

Power	Slope	Intercept
750 W	0.04	43
1000 W	0.27	-33

Table 4.7. Slope and intercept values from trendline fit to mushy zone areas

Power	Slope	Intercept
750 W	0.05	39
1000 W	0.12	42

There is a significant difference in slope caused by the increase in power, while there is also a large effect on the area of the just solidified zone in comparison to mushy zone indicating significantly large heat buildup in the sample. The negative intercept cannot be treated as the starting size of the just solidified region but gives us an understanding of the latter layers being significantly hotter than portions of initial layer. The comparison of slopes of the trend-lines for mushy zone also states that the increased power has created a steeper ascension in the area through the deposition.

Experiments by varying the power were repeated on short samples. The difference between the previous experiments and this batch is that the deposition track is smaller (13.5 mm) than the previous depositions (27 mm). The same four layer deposition procedure at 750 W and 1000 W was performed and the output areas are as plotted in Figure 4.11 and Figure 4.12, respectively.

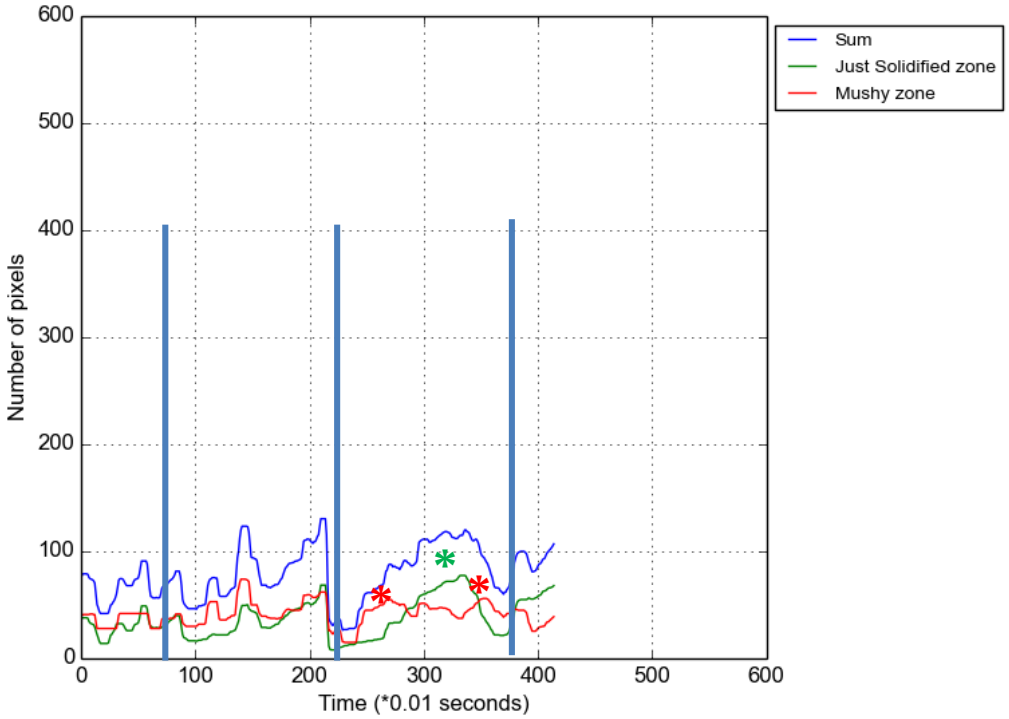

Figure 4.11. Areas of regions of interest at 750W deposition on a shorter deposition track (Stars indicate peaks due to geometry of deposition)

The blue lines indicate the locations where the laser was turned off and the direction of deposition was reversed, and the red and green asterisks indicate the location where a significant drop and rise of mushy zone and just solidified zone can be visualized (Figures 4.11 and 4.12). In the case of 750 W deposition not all layers of deposition have effectively been captured (owing to low signal). However just like in the previous set of experiments there is a rise in the signal to realize the heat variation caused due to free edges.

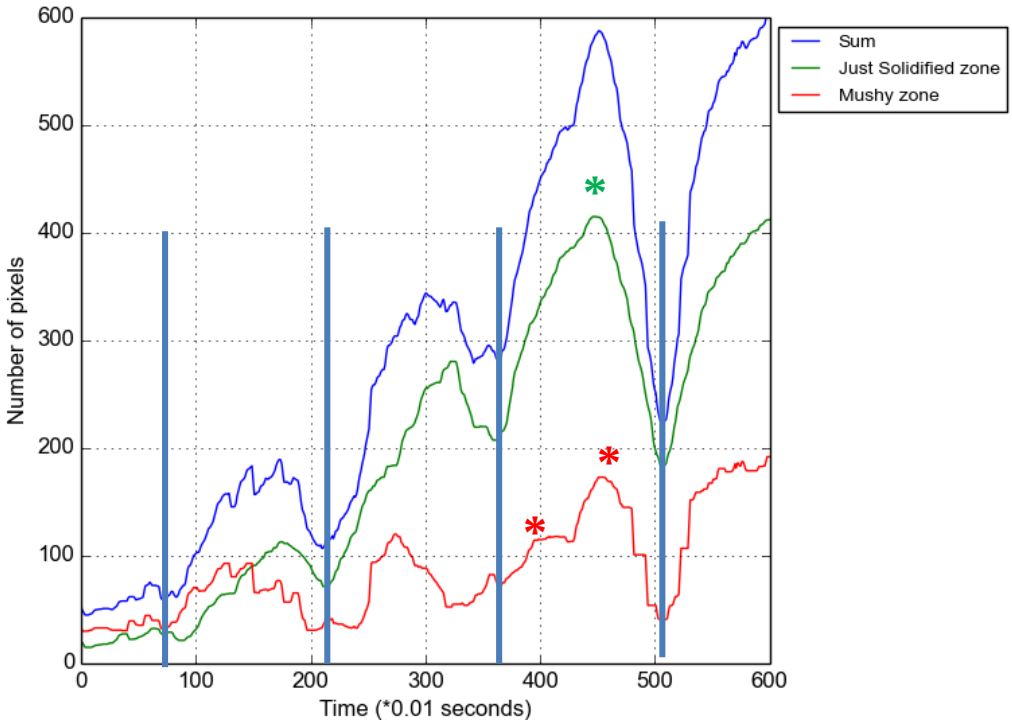

Figure 4.12. Areas of regions of interest at 1000 W on a shorter deposition track (Stars indicate peaks due to geometry of deposition)

Slope and intercept data from fitting a trend-line to the regions of interest are as detailed in Tables 4.8 and 4.9.

Table 4.8. Slope and intercept values from trendline fit for just solidified region

Power	Slope	Intercept
750 W	0.08	19
1000 W	0.7	-37

Table 4.9. Slope and intercept values from trendline fit for mushy zone

Power	Slope	Intercept
750 W	0.02	5
1000 W	0.28	8

There is a significant difference in slope similar to the case of the longer deposition track. The intercept of just solidified region is negative just as in the previous case. No conclusive insight can be attained from the intercept values of mushy zone. This could be due to the lower energy input, when compared to the long (26 mm) deposition track wherein only approximately half the amount of energy was input into the system in this case.

4.4. REPEATABILITY

Analyses of repetitions of all experiments yielded similar output in terms of the evaluated mushy zone area. Although the scaling wasn't same, the trend in variation was similar. The evaluated area from repetitions for one of the experiments is as shown in Figure 4.13. The plots in Figure 4.13 are not in sync. The drops and rises corresponding to laser powering on are at an arbitrary yet constant phase difference. Though there is difference in values of each peak the variation follows a pattern. The difference in values could be due to the variation in sample setup hence proving the system to be sensitive to even minute changes in setup.

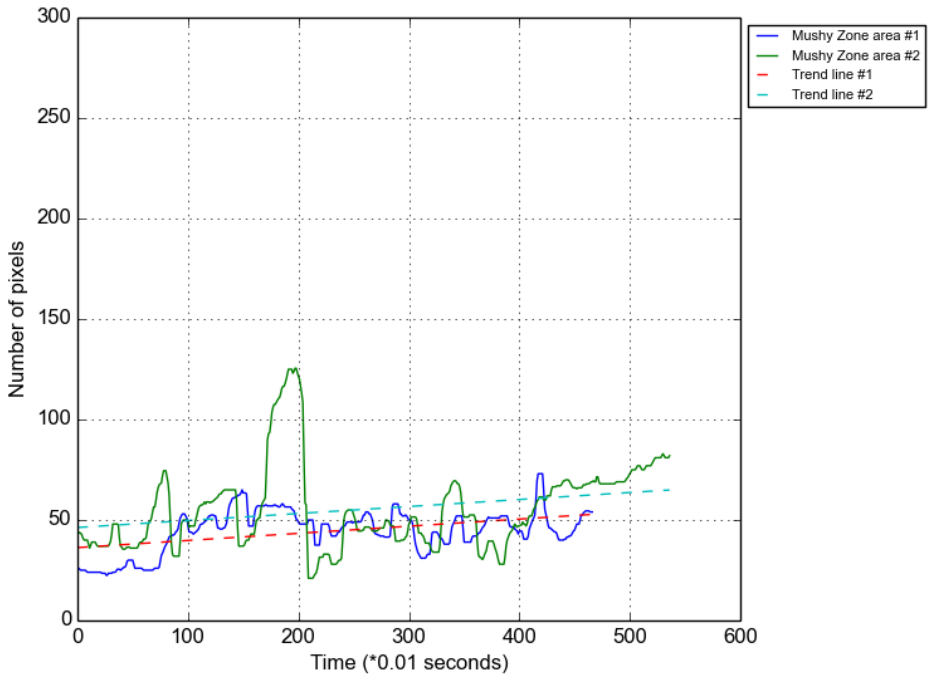

Figure 4.13. Area of mushy zone evaluated from repetitions of same experiment

4.5. CONCLUSIONS

The experimentation involved successful deposition and analysis of four layers of SS 304 on thin-wall shaped SS 304 substrates. The deposition was captured using a FLIR IR camera and the acquired thermal data was processed to identify regions corresponding to melt-pool, material in freezing range and around solidus temperature on the deposit during deposition. The experimentation was aimed at identifying the effect of height, track length and power during deposition. The effect of height was identified by performing deposition on thin-wall shaped substrates with varying thin-wall heights. A definite variation in the areas corresponding to mushy zone and just solidified region was observed. Larger areas of mushy zone and just solidified zone were seen to form during deposition with increasing height. The effect was further qualitatively understood by performing a trend-line analysis, the slope and intercept from the fit were observed to realize the effect of increasing height. As the height increased the area of mushy zone and just solidified region were noticed to increase with increasing slope. The effect of power

was realized by performing depositions at 750 and 1000 W. The higher power yielded higher areas of mushy and just-solidified zones during the course of deposition. Slope and intercept values attained from trend-line analysis showed a steeper ascension in areas of mushy zone and just solidified region with increasing power. There was a vast increase in the slope values with increasing power signifying increasing heat buildup in the deposit. Similar effects were noticed on substrates with smaller track length when tested for power variation. In spite of lower energy input, traits similar to longer track depositions were neatly picked up by analysis methodology. The repeatability of the analysis was tested by comparing results from repetitions of experiments. Though the value at an instance varied, variation trends were seen to be significantly similar.

5. FUTURE WORK

The successful interpretations obtained from the current analysis include decoupling the thermographic data to estimate and size the mushy zone and just solidified zone. These estimates are useful in realizing solidification and calculating build history. Monitoring the centroids and extremes of these regions can help track the solidification through the deposition. These skills will be utilized in studying the fabrication of functionally graded materials. Build rates and layer heights would be calculated to realize remelting and estimate material grading during deposition. The developed methodology would be used as a model validation and process monitoring tool for further analysis of the fabricating technique i.e. LMD.

BIBLIOGRAPHY

[1] Jyoti Mazumdar Lijun Song, "Advances in Direct Metal Deposition," NSF-IUCRC-2010, ppt, University of Michigan.

[2] M.L. Griffith D. M. Keicher, C. L. Atwood, J. A. Romero, J. E. Smugeresky., L. D. Harwell, D. L. Greene, "Free Form Fabrication of Metallic Components Using Laser Engineered Net Shaping (LENSTM)," Proc. of the Solid Freeform Fabrication Symp. (Austin, TX: The University of Texas at Austin), p. 125.

[3] Dave M. Keicher and John M. Smugeresky, "The Laser Forming of Metallic Components Using Particulate Materials," JOM, 49 (5) (1997), p. 51.

[4] Clint Atwood, Michelle Griffth, Lane Harwell, Eric Schlienger, Mark Ensz, John Smugeresky, Tony Romero, Don Greene, Daryl Reckaway, "Laser Engineered Net Shaping (LENS™): A Tool for Direct Fabrication of Metal Parts," Proc. Of ICALEO '98, (Orlando, Fl: Laser Institute of America, 1999), p. E-1.

[5] Eric Schlienger, Duane Dimos, Michelle Griffith, Joseph Michael, Mike Oliver, Tony Romero, John Smugeresky, "Near Net Shape Production of Metal Components Using LENS™," Proc. of the Third Pacific Rim International Conference on Advanced Materials and Processing, (Warrendale PA: TMS, 1998), p. 1581

[6] Nannan Guo, Ming C. Leu, "Additive manufacturing: technology, applications and research needs," Front. Mech. Eng. 2013, 8(3): 215–243

[7] Diller, T., Sreenivasan, R., Beaman, J., Bourell, D., LaRocco J., "Thermal model of the build environment for polyamide powder selective laser sintering," Proceedings of the 21st Annual International Solid Freeform Fabrication Symposium (SSF 2010), The University of Texas at Austin 2010, pp. 539-548.

[8] Sauer, A. "Optimierung der Bauteileigenschaften beim Selektiven Lasersintern von Thermoplasten," PhD thesis; University of Duisburg-Essen, 2005.

[9] Emmanuel Rodriguez, Francisco Medina, David Espalin, Cesar Terrazas, Dan Muse, Chad Henry, Eric MacDonald, and Ryan B. Wicker; " Integration of a Thermal Imaging Feedback Control System in Electron Beam Melting," Proceedings of the 23rd Annual International Solid Freeform Fabrication Symposium (SSF 2012): The University of Texas at Austin 2012, pp. 945-961.

[10] Liu JC, Li LJ, "Effects of process variables on laser direct formation of a thinwall," Opt Laser Technol 39(2):231-236. (2007)

[11] Cao X, Xiao M, Jahazi M, Fournier J, Alain M, "Optimization of processing parameters during laser cladding of ZE41A-T5 magnesium alloy castings using Taguchi method," Mater Manuf Processes. 23(3-4):413-418. (2008)

[12] Song L, Bagavath-Singh V, Dutta B, Mazumder J "Control of melt pool temperature and deposition height during direct metal deposition process," Int J Manuf Technol 58:247-256(2012)

[13] Kovacevic R. Zhang Y M, (1997) "Real-time Image processing for monitoring of free weld pool surface," Jour of Manufac Scie and Engi 119:161-169 (2012)

[14] Zhang Y, Zhang C, Tan L, Li S "Co-axial monitoring of fibre laser lap welding of Zn-coated steel sheets using an auxiliary illuminant Optics," Optics & Laser Technology, 50:167-175 (2013)

[15] Huang R S, Liu L M, Song G, "Infrared temperature measurement and interference analysis of magnesium alloys in hybrid laser-TIG welding process," Materials Science and Engineering, A 447:239-243,(2007)

[16] Lin L, "A comparative study of ultrasound emission characteristics in laser processing," Applied Surface science, 186:604-610,(2002)

[17] Gao J, Qin G, Yang J He J, Zhang T, Wu C, "Image processing of weld pool and keyhole in Nd:YAG laser welding of stainless steel based on visual sensing," Trans. Nonferrous Met. Soc. China,21:423-428 (2011)

[18] Saeed G, Zhang Y M, "Weld pool surface depth measurement using a calibrated camera and structured light," Meas. Sci. Tech, 18:2570-2578,(2007)

[19] Luo M, Shin Y C, "Vision-based weld pool boundary extraction and width measurement during keyhole fiber laser welding," Optics and Lasers in Engineering,64:59-70, (2015)

[20] Karnati S, Sparks T, Liou F, "Vision-based process monitoring for laser metal deposition processes," Proceedings Solid Freeform Fabrication symposium 88-94 (2013)

[21] Emissivity values as extracted on May 2014 from, http://www.raytek.com/Raytek/en-r0/IREducation/EmissivityTableMetals.htm, http://www-eng.lbl.gov/~dw/projects/DW4229_LHC_detector_analysis/calculations/emissivity2.pdf

[22] Edge detection techniques as extracted on May 2014, http://www.owlnet.rice.edu/~elec539/Projects97/morphjrks/laplacian.html

[23] Multi-dimensional image processing python libraries, https://docs.scipy.org/doc/scipy-0.15.1/reference/ndimage.html

VITA

Sreekar Karnati was born and brought up in Hyderabad, India. He obtained his undergraduate degree in Manufacturing Science and Engineering from Indian Institute of Technology, Kharagpur, India in 2012. During his senior year, he worked on the project titled, “A Molecular mechanics investigation of the mechanical properties of functionalized CNT-epoxy composites” under the supervision of Dr. Baidurya Bhattacharya. His work involved developing a molecular dynamics model of the CNT epoxy composite and evaluating its mechanical properties through simulation. After his graduation, in fall 2012 he started graduate studies in Manufacturing Engineering at Missouri University of Science and Technology, Rolla, Missouri.

During his course of study, he has worked on fabrication and characterization of advanced materials namely, functionally graded materials, high entropy alloys and structurally amorphous materials via laser metal deposition. He received his M.S. degree in Manufacturing Engineering from Missouri University of Science and Technology in May, 2015.